

Influence of friction between layers of mechanically lined pipes on collapse resistance

Original

Influence of friction between layers of mechanically lined pipes on collapse resistance / Echer, Leonel; Clarke, Thomas Gabriel Rosauo; Groth, Eduardo Becker; Dias, Allan Romário De Paula; Iturrioz, Ignacio; Kuhn, Matheus Freitas; Ubessi, Cristiano Joao Brizzi; Carvalhal, Rodrigo Do Nascimento; Ilstad, Håvar; Kaspary, Tiago; Berntsen, John Fredrick. - ELETTRONICO. - 22:(2024). (Rio Oil & Gas (ROG.e) Rio de Janeiro (Brasile) 23/09/2024 -- 26/09/2024) [10.48072/2525-7579.roge.2024.4052].

Availability:

This version is available at: 11583/3002176 since: 2025-07-28T16:11:09Z

Publisher:

Instituto Brasileiro de Petróleo e Gás (IBP)

Published

DOI:10.48072/2525-7579.roge.2024.4052

Terms of use:

This article is made available under terms and conditions as specified in the corresponding bibliographic description in the repository

Publisher copyright

(Article begins on next page)

Influence of friction between layers of mechanically lined pipes on collapse resistance

Influence of friction between layers of mechanically lined pipes on collapse resistance

Leonel Echer , Thomas Gabriel Rosauo Clarke , Eduardo Becker Groth , Allan Romário de Paula Dias , Ignacio Iturrioz, Matheus Freitas Kuhn, Cristiano Joao Brizzi Ubessi , Rodrigo do Nascimento Carvalho , Håvar Iltstad, Tiago Kaspary, John Fredrick Berntse

Abstract:

Mechanically lined pipes (MLP) are characterized by their two-layer structure consisting of an external carbon steel pipe responsible for the mechanical strength of the component and an inner pipe with a thinner wall made of a corrosion-resistant alloy (CRA). There is no metallurgical bond between these layers, meaning that their interaction is mainly defined by contact mechanisms influenced by the surface preparation, material properties and hydraulic expansion manufacturing processes used. This leads to difficulties in determining the operating limits of these pipes. This work focuses on the effects of friction between the layers of MLP on its resistance to collapse due to external pressure. Currently, the criteria established by the DNV-ST-F101 standard consider the contribution of the CRA layer in the collapse pressure calculation only for clad pipes (where there is metallurgical bonding between the layers), and there is no specific calculation procedure defined for MLP. In order to contribute to the current design codes for these components, this work aims to measure the friction coefficient between the layers of an MLP, to demonstrate the effect of this parameter on the collapse resistance of MLP. For this purpose, an experimental apparatus was assembled to obtain the static friction coefficient (μ_s) of samples extracted from different production batches of MLP. Finite element modelling results will be used to illustrate the importance of having accurate measurements of this parameter when establishing the collapse pressure of MLP.

Keywords: Mechanically lined pipes; Collapse capacity; Numerical simulation; friction coefficient; testing method

Os tubos revestidos mecanicamente (MLP) caracterizam-se por sua estrutura bimetálica composta por um tubo externo de aço carbono responsável pela resistência mecânica do componente e um tubo interno de parede mais fina confeccionado em liga resistente à corrosão (CRA). Não existe ligação metalúrgica entre estas camadas, o que significa que a sua interação é definida principalmente por mecanismos de contato influenciados pela preparação da superfície, propriedades do material e processos de fabricação de expansão hidráulica utilizados. Isto leva a dificuldades na determinação dos limites de operação destes tubos. Este trabalho enfoca os efeitos do atrito entre as camadas do MLP na sua resistência ao colapso devido à pressão externa. Atualmente, os critérios estabelecidos pela norma DNV-ST-F101 consideram a contribuição da camada CRA no cálculo da pressão de colapso apenas para tubos cladeados (onde há ligação metalúrgica entre as camadas), e não há procedimento de cálculo específico definido para MLP. Visando contribuir com os atuais códigos de projeto para estes componentes, este trabalho tem como objetivo medir o coeficiente de atrito entre as camadas do MLP, para demonstrar o efeito deste parâmetro na resistência ao colapso do MLP. Para tanto, foi montado um aparato experimental para obtenção do coeficiente de atrito estático (μ_s) de amostras extraídas de diferentes lotes de produção de MLP. Os resultados da modelagem de elementos finitos serão usados para ilustrar a importância de ter medições precisas deste parâmetro ao estabelecer a pressão de colapso do MLP.

Palavras-chave: Mechanically lined pipes; Colapso; Dutos submarinos; atrito; Pipeline.

Received: September 8th, 2024 | **Accepted:** July 7th, 2024 | **Available online:** September 23th, 2024

Article n°: 4052

DOI: <https://doi.org/10.48072/2525-7579.rog.e.2024.4052>

1. Instituto SENAI de Inovação em Engenharia de Polímeros. Polímeros Estruturais. BRASIL. E-mail: leonel.echer@senairs.org.br. (<https://orcid.org/0000-0003-0353-8941>). 2. Universidade Federal do Rio Grande do Sul, UFRGS/LAMEF. Metalurgia. BRASIL. E-mail: tclarke@demet.ufrgs.br. (<https://orcid.org/0000-0001-6975-2911>). 3. Universidade Federal do Rio Grande do Sul, UFRGS/LAMEF. LAMEF. BRASIL. E-mail: eduardo.groth@ufrgs.br. (<https://orcid.org/0000-0002-0017-6554>). 4. Universidade Federal do Rio Grande do Sul, UFRGS/LAMEF. BRASIL. E-mail: allan.dias@ufrgs.br. (<https://orcid.org/0000-0002-7430-6569>). 5. Universidade Federal do Rio Grande do Sul, UFRGS/DEMEC. BRASIL. E-mail: ignacio.iturrioz@ufrgs.br. 6. Universidade Federal do Rio Grande do Sul, UFRGS/LAMEF. BRASIL. E-mail: matheus.kuhn@ufrgs.br. 7. Universidade Federal do Rio Grande do Sul, UFRGS/DEMEC. Engenharia Mecânica. BRASIL. E-mail: cristiano.ubessi@ufrgs.br. (<https://orcid.org/0000-0002-7516-7409>). 8. Equinor Brasil. Research & Development. BRASIL. E-mail: rodca@equinor.com. (<https://orcid.org/0009-0004-5566-8128>) 9. Equinor ASA. NORUEGA. E-mail: hil@equinor.com. 10. Cladtek do Brasil. BRASIL. E-mail: tiago.kaspary@cladtek.com. 11. Equinor ASA. TDI. NORUEGA. E-mail: jfbe@equinor.com. (<https://orcid.org/0009-0002-4551-3099>)

1. Introduction

The collapse of submarine pipelines can have massive economic and environmental impacts. Therefore, knowledge of their mechanical behaviour under external pressure is essential for their design, fabrication, installation, and operation in deepwater exploration. Industrial and academic players have spent considerable resources investigating a wide range of problems in this field. International standards have been published and are reviewed periodically in order to establish safety parameters, design concepts and construction premises of subsea pipelines. However, the increasing depth of installation sites, the constant need for optimisation, and the aggressive nature of the environment, lead to constant practical developments and improvements. An example of this is the use of corrosion-resistance alloys (CRA) to protect the internal surface of the pipes, resulting in a bimetallic structure commonly called mechanically-lined pipe (MLP).

It has been shown, i.e. Giordani, G. et.al. (2022), that the CRA liner provides additional mechanical resistance to collapse in MLP, and this means that under certain circumstances the applicable standards have become too conservative in their assumptions and in the safety factors recommended for such pipelines. This paper aims at assessing the influence of the friction coefficient between the CRA liner and backing steel (BS) on the collapse resistance of MLP. For this, an experimental apparatus was developed to measure friction coefficient values for a batch of commercial pipes with Inconel liners. Finite element models were then used to understand how different levels of friction can affect the collapse capacity of MLP samples with different diameter-to-wall thickness ratios (D/t).

1.1. Motivation and objectives

The interface interactions between backing steel and liner are determined by surface and contact conditions, that is, friction and gripping forces that arise due to stress gradients developed during the hydroexpansion process that is commonly used in MLP manufacturing. Accurate measurement of the friction coefficient between the layers can therefore help to understand these effects. Hence, the objectives of the present paper are:

- To present the testing framework for the determination of friction coefficient.
- To show the testing setup detailing each aspect of the mechanical sliding tests.
- Present a simulation strategy for the buckling capacity of MLP based on the arc length method.
- To discuss results for the friction coefficient and its effects on the collapse capacity of MLP over a range of D/t .

2. Materials and methods

The experimental framework adopted in the present analysis was based on the sliding friction principle, which consists of measuring the sliding resistance (Blau, 2001) between solid bodies by sliding one body over the surface of another while computing the force that opposes the sliding direction. Such a reaction force is known as F_{μ} , friction force, which can be directly related to the friction coefficient μ . This approach was chosen due to its characteristic of combining simplicity and reliability (Hasan, 2021). The current section will present the detailed aspects of the experimental procedure for friction measurement, and of the finite element simulations that were used to verify the influence of friction on collapse capacity of pipes with different D/t ratios.

2.1. Material preparation

In the present experimental analysis, the bodies used as sledge and plate were CRA and BS pipe segments (slabs), respectively. The specimens were retrieved from a sector of the pipelines through straight cuts, longitudinal to the pipe, as illustrated in Figure 1. Specimens had a total length of 400mm and 80 mm wide (which roughly corresponds to 1/8 of the perimeter of the pipe). Figure 1a illustrates general sample dimensions before the pipe cutting. The lateral cuts, which extend along the sample's length, were aligned with the axial direction, resulting in slab-like samples with lateral faces perpendicular to the circumferential direction, *i.e.*, tangential. It is important to note that in order to allow space for the CRA to slide over the BS during the test, the CRA slabs were cut in half-length, reducing its extension to 200mm. The sampling configuration is presented in Figure 1b. It should be clear that sectioning the pipes in this way effectively removes the gripping force that results from the hydroexpansion manufacturing process of the MLP.

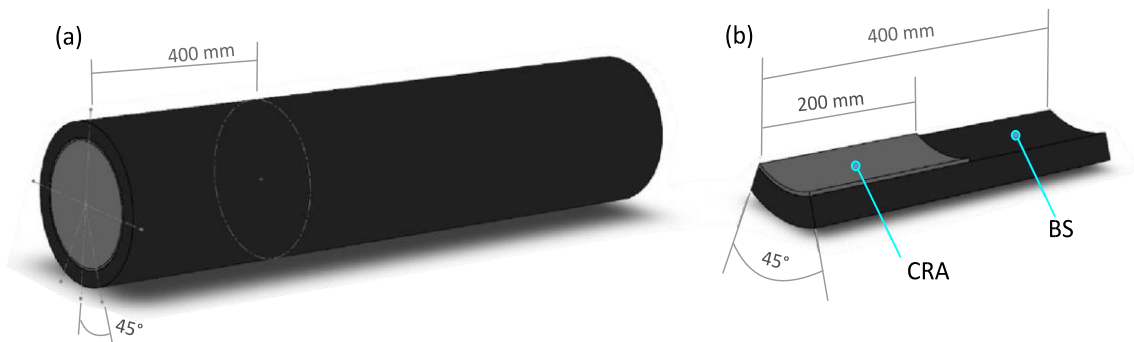


Figure 1: Specimen preparation: a) sample extraction from the pipe, and b) sample ready for testing.

2.2 Experimental setup for friction measurements

To carry out experimental tests using a setup similar to the one shown in Figure 2, a custom workbench was designed. The workbench and test equipment were connected to a universal testing machine (INSTRON 5585H) with the testing configuration as illustrated in Figure 3. Certain aspects of the testing apparatus and details were adapted to accommodate the unique geometries of the specimen, such as the pipe sector with non-flat inner and outer surfaces. These adaptations will be discussed in detail in the following section.

The pulley and cable components were arranged to be as stiff to prevent energy from being stored in the system during operation. Additional mass was placed on top of the CRA slab to ensure better interface interaction during the sliding of the CRA over the BS. This measure also aimed to prevent stick-slip motion behaviour, which produces additional noise in the computation of friction force as described in (Worden, Wong, Parlitz, Hornstein, Engster, Tjahjowidodo, Al-Bender, Rizos, and Fassois, 2007). Weight standard blocks typically used for calibrating load cells were used as additional mass. Therefore, the additional mass was calculated from the total weight of the disks added during each test, with each disk weighing 4,535.92g.

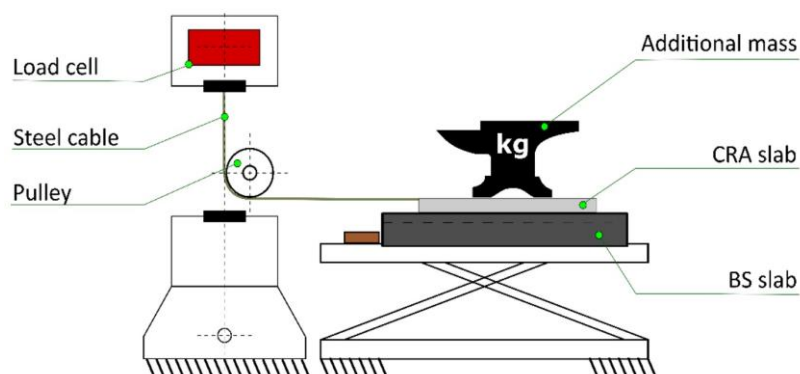


Figure 2: Experimental setup adopted in the friction coefficient testing.

The machine is attached to the test specimen by a steel cable glued to the CRA slab in place using epoxy resin. Because the top and bottom surfaces of the specimens were not flat, modelling clay was applied over the CRA slab to ensure a perfect coupling with the additional mass disks to guarantee the weight distribution on the specimen surface.

The friction coefficient was computed at any given moment during the sliding tests and estimated through Equation 1. Thus, μ was directly computed using Equation 1 and assuming the gravity as 9.8m/s^2 . All sliding tests were performed using displacement control. After conducting several pilot tests to define the best testing parameters, the crosshead speed of the machine, $\dot{u} = 0.5\text{mm/min}$ was chosen as optimal. Also, the loading cell used on all tests had a maximum capacity of 200kN. From

each test, the curve force versus displacement (or time) was retrieved, $F_{Frict} \times u$. All curves were submitted to signal processing to compute the static friction coefficient μ for each material/test.

$$\mu = \frac{F_{fric}}{g \cdot (m_{CRA} + m_{add})} \quad (1)$$

A picture of the test setup is depicted in Figure 3a illustrating both CRA and BS slabs bonded each other and attached to the test machine. The raw data read from the test machine is depicted in Figure 3b with the point of interest for the static friction coefficient indicated by number 1. Number 2 indicates the typical signal observed in the stick-slip phenomenon, commonly observed in this test.

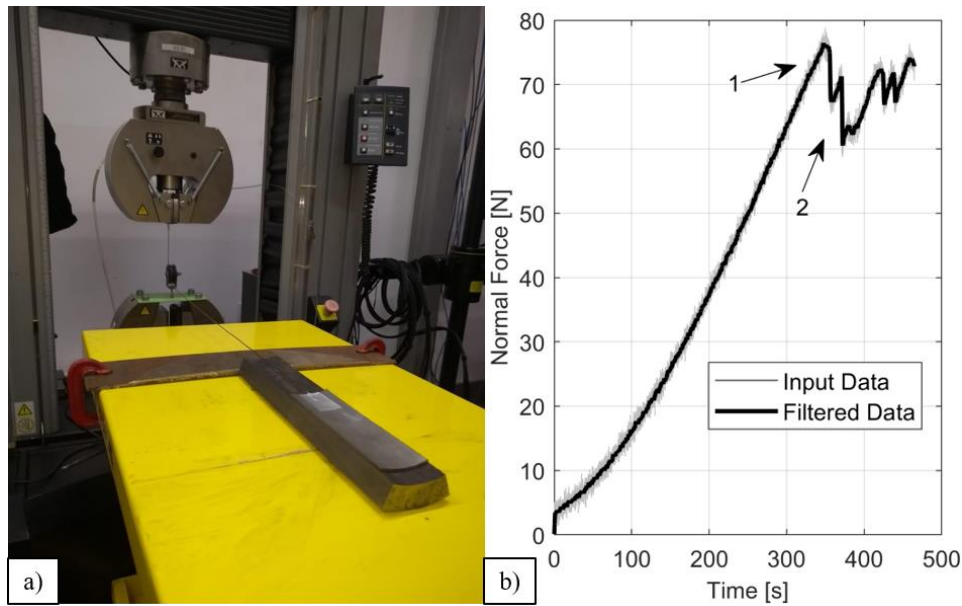


Figure 3: a) Sliding test execution and b) displacement versus friction force: 1 – static friction coefficient, 2 – stick-slip signal.

2.3 Friction measurements data analysis

The curves obtained from the sliding tests were submitted to a low-pass filter to suppress spurious signal peaks. *IIR*, *FIR*, *Savitzky-Golay*, and *Butterworth* filters were tested. The latter provided the best results with minimal computation cost; thus, the Butterworth low-pass filter (Selesnick and Burrus, 1998) was adopted. After applying linear regression to each testing batch, a descriptive statistical analysis was conducted to identify any potential outliers. To measure the interquartile range (IQR), the quartile values that are widely adopted in the literature were used, that is, the median is equal to 50%, Q3 is equal to the upper 75%, and Q1 is equal to the lower 25%.

2.4 Collapse simulation

The influence of friction on the collapse capacity of MLP was evaluated through a parametric finite element analysis study, within a D/t range that is commonly used in the offshore oil exploration industry. The simulations assumed the structure, mesh and boundary conditions validated and used in Giordani, G et.al. (2022) and are summarized in Figure 4.

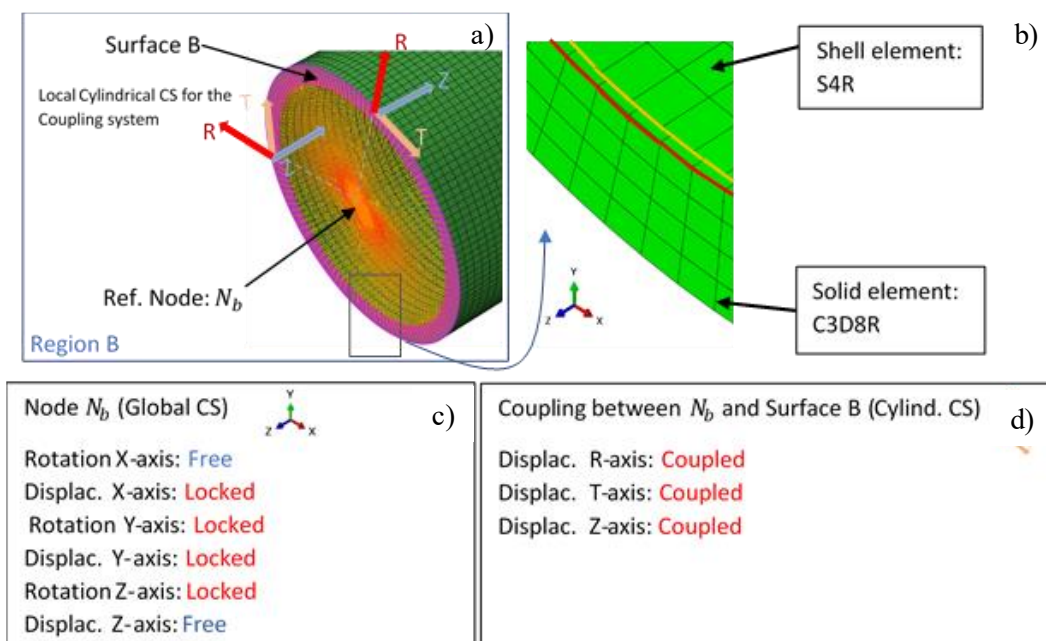


Figure 4: a) and b) FEM model structure, coordinate system and mesh from Giordani, G et.al. (2022); c) and d) boundary conditions.

The models were built as two cylinders concentrically mounted in contact, with an endcap at the pipe end (Figure 4a). The pipe was discretized by linear elements with reduced integration, and the CRA liner by shell elements (Figure 4b). The endcap was defined by the application of boundary conditions to the reference node N_b coupled to the surface nodes. Finally, the buckling capacity was estimated using the Riks algorithm to obtain the maximum external pressure sustained by the solid in the hydrostatic load conditions.

The material model was obtained through the Ramberg-Osgood power law function assuming the parameters listed in Table 1.

Table 1: Ramberg-Osgood parameters.

Material	E [GPa]	Poisson [-]	Sy [MPa]	Exponent (n)	Yield Offset (α)
Liner	195	0.30	170	3.125	4.183
Steel	207	0.30	450	13.28	1.206

3 Results

3.2 Friction

The friction coefficients between liner and carbon steel were measured for several pipe joints collected from different production batches at the pipe mill in order, and the mean friction coefficient resulted in 0.49. The summary of all friction coefficients measured in this test scheme is listed in Table 2, in which it is possible to observe they range between 0.41 and 0.627. The statistical distribution of these measures is illustrated in the boxplots shown in Figure 5. The roughness parameter Ra, which is listed in Table 2 for BS and CRA liner, represents the average surface roughness (i.e., the average difference between peaks and valleys) for the length of the measurement performed. This measurement is representative of the general condition of the surface.

Table 2: Summary of friction coefficients measurement results.

Specimen	Friction coefficient	Ra_{CRA}	Ra_{BS}
33467	0.56	6.83	7.07
33469	0.43	4.86	8.01
33470	0.50	5.30	6.74
33472	0.40	4.45	8.57
33513	0.42	5.36	5.98
Mean	0.490	4.44	8.23
Std. Dev.	0.028	0.97	1.79

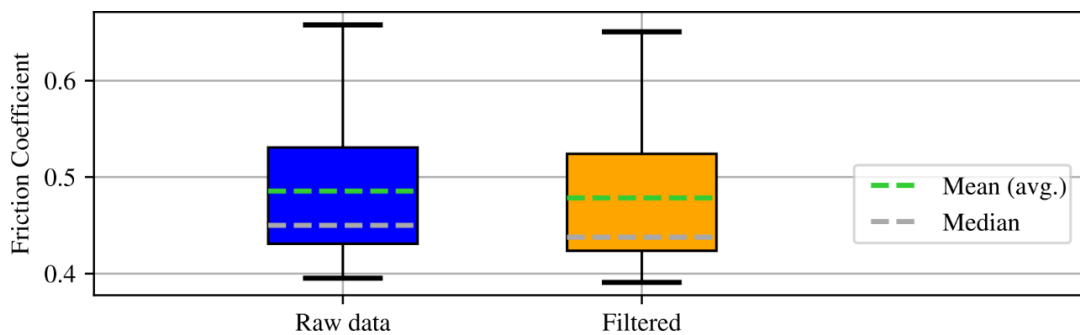


Figure 5 - Statistical distribution of the friction coefficients measured in several pipe joints.

3.3 Collapse simulation

Using the model settings previously described, it was possible to run the models listed in Table 3, and results are displayed in Figure 6. In absolute terms, the difference in collapse pressure for a pipe with no friction and with increasing values of friction coefficient is small; the highest value of absolute

gain for a pipe with maximum friction compared to the case with no friction is 6MPa for $D/t=8$. For a pipe with $D/t=10$ the absolute gain would be of 4MPa, and for all other cases it would be 2MPa. However, up to 5% gain in collapse pressure is achieved when the highest friction coefficient value is used relative to the case with no friction for pipes with high D/t ($=22.5$). For the other D/t values, the percentage gain in collapse pressure is between 3% and 4.4%.

Table 3- Parametric study for the effect of friction on the collapse pressure.

OD [mm]	w.t. [mm]	w.t. _{liner} [mm]	D/t	Collapse pressure [MPa] for $\mu =$						Maximum absolute gain rel. $\mu =0$ [MPa]	Maximum % gain rel. $\mu =0$
				0	0.2	0.4	0.6	0.8	1		
220	27.5	3.0	8	156	159	160	161	161	162	6	3.8
220	22	3.0	10	115	117	118	118	118	119	4	3.5
220	17.6	3.0	12.5	85	86	87	87	88	88	3	3.5
220	14.7	3.0	15	67	67	68	68	69	69	2	3
220	12.6	3.0	17.5	54	55	55	56	56	56	2	3.7
220	11	3.0	20	45	46	46	47	47	47	2	4.4
220	9.878	3.0	22.5	38	39	39	39	40	40	2	5.3

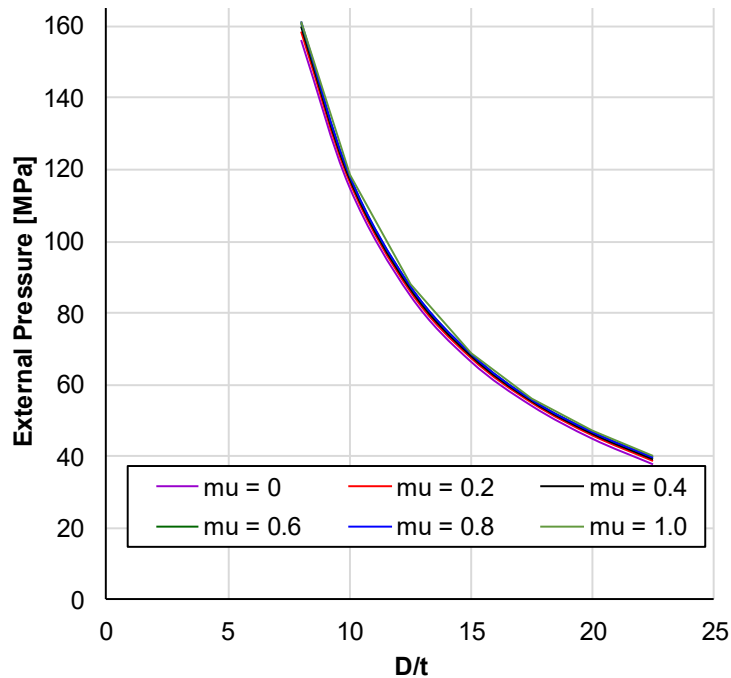


Figure 6: Collapse capacity for the simulated pipes over the D/t range analysed.

4. Final remarks

From the sequential testing of different pairs of material (BS and CRA slabs), the average friction coefficient μ_{avg} was computed as 0.494 for the specimens retrieved from MLP pipes. This value was defined after the signal processing and statistical analysis of several $F_{Fric} \times u$ curves obtained through sliding tests. Finite element results show that pipes with low D/t are the ones that benefit the most from having high friction between the layers in terms of absolute gain in collapse pressure, although the gain is small (maximum of 6MPa for D/t=8). In terms of percentual gain relative to the collapse pressure of a pipe with no friction, pipes with high D/t (above 20) would benefit the most from having high friction (up to 5.3% for D/t=22.5). It should be clear that these results express the influence of friction on collapse pressure under a limited set of conditions, and this issue will be further explored in future work.

5. Acknowledgement

The authors would like to thank ANP (Agência Nacional de Petróleo, Gás Natural e Biocombustíveis) and EMBRAPPII (Empresa Brasileira de Pesquisa e Inovação Industrial) for funding this project, and Vallourec Tubular Solutions (VTS) for important discussions and for providing the infrastructure and key personnel that allowed the full-scale testing activities of this project. Professor Thomas Clarke would like to further acknowledge grants received from CNPq (PQ programs), and from CAPES-PROEX through PPGE3M (Programa de Pós-Graduação em Engenharia de Minas, Metalúrgica e de Materiais).

Referências

- Bhushan, B. (2024). Fundamentals of Tribology and Bridging the Gap Between the Macro- and Micro/Nanoscales (Vol. 10).
- Blau, P. J. (2001). The significance and use of the friction coefficient, *Tribology International*. *Tribology International*, 34(9), 585-591. [https://doi.org/10.1016/S0301-679X\(01\)00050-0](https://doi.org/10.1016/S0301-679X(01)00050-0)
- Det Norske Veritas (Ed.). (2021). Submarine Pipeline System. In DNV-ST-F101. DNV. <https://www.dnv.com/oilgas/download/dnv-st-f101-submarine-pipeline-systems>
- Hasan, A. (2021). Experimental analysis of the co-efficient of static friction between different pairs of surfaces using horizontal plane apparatus. *Journal of Physics: Conference Series*, 1(1950), 012033. <https://doi.org/10.1088/1742-6596/1950/1/012033>
- Propagation pressure collapse in conventional pipelines and MLPs: Numerical investigation. (2022). *Marine Structures*, 83(103192), 103192. <https://doi.org/10.1016/j.marstruc.2022.103192>.
- Selenick, I., & Burrus, C. (1998). Generalized digital Butterworth filter design. *IEEE Transactions on Signal Processing*, 46(1), 1688-1694.
- Vasilikis, D., & Karamanos, S. A. (2009). Stability of confined thin-walled steel cylinders under external pressure. *International Journal of Mechanical Sciences*, 51(2009), 21-32. <https://doi.org/10.1016/j.ijmecsci.2008.11.006>
- Vedeld, K., Osnes, H., & Fyrileiv, O. (2023). Analytical expressions for stress distributions in lined pipes: Axial stress and contact pressure interaction. *Marine Structures*, 26(2012), 1-26. <https://doi.org/10.1016/j.marstruc.2011.12.003>
- Veldet, K., Osnes, H., & Fyrileiv, O. (2012). New interpretations of gripping force tests for lined pipes. *Marine Structures*, 29(2012b), 152-168. <https://doi.org/10.1016/j.marstruc.2012.10.004>
- Worden, k., Wong, X. T., Parlitz, U., Hornstein, A., Engster, D., Tjahjowidodo, T., Bender, Al, Rizos, D. D., & Fassois, S. D. (2007). Identification of pre-sliding and sliding friction dynamics: Grey box and black-box models. *Mechanical Systems and Signal Processing*, 21(1), 514-534. <https://doi.org/10.1016/j.ymsp.2005.09.004>

Access all Papers

biblioteca.ibp.org.br

